

## Benchmark Tests for Strong Ground Motion Simulations (Part 9: Theoretical Methods, Step 5 & 6)

MATSUMOTO, Toshiaki<sup>1\*</sup>, HISADA, Yoshiaki<sup>1</sup>, NAGANO, Masayuki<sup>2</sup>, NOZU, Atsushi<sup>3</sup>, ASANO, Kimiyuki<sup>4</sup>, MIYAKOSHI, Ken<sup>5</sup>

<sup>1</sup>Kogakuin University, <sup>2</sup>Tokyo University of Science, <sup>3</sup>The Port and Airport Research Institute, <sup>4</sup>Disaster Prevention Research Institute, <sup>5</sup>Geo-Research Institute

We have been conducting a series of benchmark tests of the strong motion simulation methods for three years since 2009. We chose the three most popular methods for this purpose: the theoretical methods (the wavenumber integration method, the discrete wavenumber method, and the thin-element method), the stochastic Green function method, and the numerical methods (the finite difference method and the finite element method). In this presentation (Part 9), we show the results of the theoretical methods for flat-layered structures in the step 5 and 6, and subsequent papers (Part 10) and (Part 11) show the results for numerical and empirical methods, respectively.

Show table 1, this table is list of Benchmark tests for the 2011 theoretical method (step 5 and 6). The step 5 and 6 use the Kanto sedimentary basin for the actual seismic sources (e.g., the 1990 West Kanagawa earthquake (M5.1) for step 5, and the 1923 Kanto earthquake (M7.9) for step 6). We selected 19 calculation points at the Kanto sedimentary basin from AIJ strong ground motion data sets, as shown figure 1. Structure models are flat-layered structures that extracted every 19 calculation points from 3D structure models.

All the results using various methods (the wavenumber integration method, the discrete wavenumber method, and the thin-layer method) generally show good agreements, as long as we use the same source and structure models. As compared with the observed records, those results generally simulate the body waves very well, but not the basin-induced surface waves.

Please check the following web site for more details.  
<http://kouzou.cc.kogakuin.ac.jp/benchmark/index.htm>

### Acknowledgements:

This project is in part supported by a research fund of Ministry of Education, Culture, Sports, Science and Technology of Japan (MEXT), and the Research Center of Urban Disaster Mitigation (UDM) of Kogakuin University. Toshiaki SATO, Nobuyuki YAMADA and Reiji KOBAYASHI, for providing us source model data.

**Keywords:** Strong Ground Motion Simulations, Benchmark Test, Theoretical Methods, Wavenumber Integration Method, Discrete Wavenumber Method, Thin Layer Method

Table 1 Benchmark tests for the 2011 theoretical method (step 5 and 6)

名称	1990年西武池袋線西武池袋駅付近の地震 (M5.1)	1990年伊豆大島近海の地震 (M6.6)	1923年関東大震災 (M7.9)
震源	136.2°E, 35.7°N	139.2°E, 34.8°N	139.7°E, 35.8°N
震源深さ	10km	10km	10km
震害	関東平野の北東部関東平野の北東部	関東平野の北東部	関東平野の北東部
震害範囲	0~50km	0~50km	0~50km
震害データ	1990年西武池袋線西武池袋駅付近の地震 (M5.1)	1990年伊豆大島近海地震 (M6.6)	1923年関東大震災 (M7.9)
出力点	19地点 (AIJデータベースから19地点をランダム抽出)		

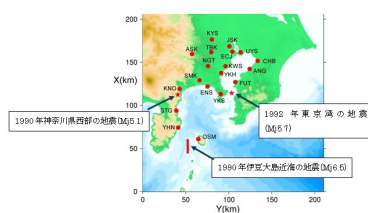


Figure 1 Location of Hypocenter and calculation points (step 5)

## Benchmark Tests for Strong Ground Motion Simulations (Part 10: Numerical Methods, Step 5 & 6)

YOSHIMURA, Chiaki<sup>1\*</sup>, NAGANO Masayuki<sup>2</sup>, HISADA Yoshiaki<sup>3</sup>, AOI Shin<sup>4</sup>, IWAKI Asako<sup>4</sup>, KAWABE Hidenori<sup>5</sup>, HAYAKAWA Takashi<sup>6</sup>, Seckin Ozgur CITAK<sup>7</sup>

<sup>1</sup>Taisei Corporation, <sup>2</sup>Tokyo University of Science, <sup>3</sup>Kogakuin University, <sup>4</sup>NIED, <sup>5</sup>Kyoto University, <sup>6</sup>Shimizu Corporation, <sup>7</sup>JAMSTEC

### 1. Introduction

We have been conducting a benchmark test for strong motion simulation methods with numerical methods (finite difference method and finite element method). During 3 years of the research period, we studied 14 problems categorized in 6 steps with various degree of complexity from a simple homogeneous model to a realistic Kanto basin model.

In step 1, we studied a homogeneous model and a two-layer model with a point source. In step 2, we studied the two-layer model with extended source models: a lateral fault and a reverse fault. (Yoshimura et al., 2011). In step 3 and 4, we considered a four-layer model, a symmetric trapezoidal basin model and an asymmetric slant-basement basin model (Yoshimura et al., 2012). In this report, we present the results of step 5 and 6 in which we considered a realistic Kanto basin model where Tokyo metropolitan area is located.

### 2. Problems for step 5 and 6

We considered a 3-dimensional Kanto basin model and the source models of 4 observed earthquakes. Six teams participated in this year. Table 1 shows the calculation conditions. Figure 1 shows the calculation domain (210km x 270km) with source model (stars or circles) and calculation sites (squares).

In step 5, we targeted 3 small or middle earthquakes: 1990 Western Kanagawa Prefecture earthquake (Mj 5.1), 1990 Near Izu-Oshima earthquake (Mj6.5) and 1992 Tokyo bay earthquake (Mj 5.7). We constructed the source models based on Sato T. et al. (1998) and Yamada and Yamanaka (2003).

We constructed the 3-dimensional Kanto Basin model based on the model proposed by The Headquarter for Earthquakes Research Promotion (2009). The grid size or element size were set so that the calculation results are effective at the frequency domain from 0 to 0.33 Hz. Participants turned in calculated velocity time history data for 19 sites.

In step 6, we targeted 1923 Kanto earthquake (Mj 7.9). The source model was constructed based on the inverted source model proposed by Sato H. et al. (2005).

### 3. An example of calculated results

Figure 2 shows the calculated Y (EW) component of velocity waves at ASK. Yoshimura calculated with FEM. Nagano, Hayakawa, Citak et al., Iwaki et al. and Kawabe calculated with FDM. In addition, Fig.2 shows Hisada's result calculated with a wave number integration method considering a flat layered model. Because ASK is a rock site, the waveform is simple. The results by FEM and FDM agree with each other. Hisada's result is similar to those results because the seismic wave mainly consists of body wave and the flat layer approximation is effective. On the other hand, at the sites on the thick sedimentary basin, the later phases induced by basin structure become dominant. Our results on sedimentary sites show generally good agreement but are not as perfect as ASK at the present moment. We are now checking reasons such as the difference of modeling of surface thin layer and are planning to revise the results.

For more details, please check <http://kouzou.cc.kogakuin.ac.jp/benchmark/index.htm>

### Acknowledgement

This project is partly supported by a research fund of Ministry of Education, Culture, Sports, Science and Technology of Japan (MEXT), and the Research Center of Urban Disaster Mitigation (UDM) of Kogakuin University. We would like to thank Dr. Toshiaki SATO, Dr. Nobuyuki YAMADA and Dr. Reiji KOBAYASHI for providing us source model data. We would like to thank Dr. Shinichi MATSUSHIMA and Dr. Robert W. GRAVES for participating in Citak's team.

### References

- 1) Yoshimura et al., AIJ J. Technol. Des. Vol.17, Mo.35, 67-72, Feb.,2011. (in Japanese)
- 2) Yoshimura et al., AIJ J. Technol. Des. Vol.18, Mo.38, 95-100, Feb.,2011. (in Japanese)
- 3) Sato T. et al., Bull. Seism. Soc. Am., Vol. 88, No1, pp.183-205, Feb., 1998.

SSS26-02

Room:304

Time:May 20 09:15-09:30

- 4) Yamada and Yamanaka, Zisin 2, Vol. 56, 111-123, 2003. (in Japanese)
- 5) The Headquarter for Earthquakes Research Promotion, 2009. [http://www.jishin.go.jp/main/chousa/09\\_choshuki/](http://www.jishin.go.jp/main/chousa/09_choshuki/)
- 6) Sato H. et al., Science, 309, 462-464, 2005.

Keywords: Fault model, Finite element method, Finite difference method, Kanto plain, Kanto earthquake, Western Kanagawa Prefecture earthquake

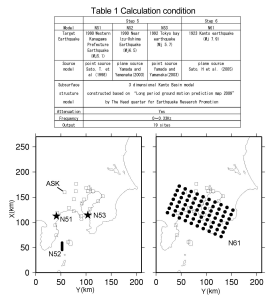


Fig.1 Calculation domain, seismic sources and output sites

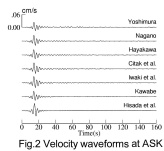


Fig.2 Velocity waveforms at ASK

## Benchmark Tests for Strong Ground Motion Simulations (Part 11:Stochastic Green's Function Method, Step 5 & 6)

KATO, Kenichi<sup>1\*</sup>, HISADA Yoshiaki<sup>2</sup>, OHNO Susumu<sup>3</sup>, NOBATA Arihide<sup>4</sup>, MORIKAWA Atsushi<sup>1</sup>, YAMAMOTO Yu<sup>5</sup>

<sup>1</sup>Kobori Research Complex Inc., <sup>2</sup>Kogakuin Univ., <sup>3</sup>Tohoku Univ., <sup>4</sup>Obayashi Co., <sup>5</sup>Taisei Co.

Benchmark tests for the strong motion simulation methods have been performed as three years project since 2009. This paper focuses on the results using stochastic Green's function method.

We have carried out simple benchmark tests in 2009; one is a point source (step 1) and the other is extended sources (step 2) in homogeneous and two-layered subsurface structures. Radiation coefficient of the source is assumed to be frequency independent, and only SH wave is considered. Site amplification is calculated assuming normal incidence of SH wave. Six groups of researchers/engineers were participated in by using their own methods/codes. Since the simple model is used in the steps 1 and 2, all the results calculated by six teams generally show good agreements to each other (Kato et al., 2011). In steps 3 (point source) and 4 (extended source), more complicated analytical conditions are considered. For example, frequency dependent radiation coefficient of the source is applied. Since oblique incidences of both SH and SV waves are considered, vertical component is also generated in addition with horizontal components. All the results of the point sources and the extended sources from five participants generally show good agreements to each other in spite of complicated analytical conditions. Synthesized amplitude shows variation in particular frequencies, because random numbers are used in generating time histories. When applying the stochastic Green's function method, this variation should be in mind (Kato et al., 2012).

In the steps 5 and 6, the Kanto sedimentary basin for the 1923 Kanto earthquake (M7.9) is considered as an actual source and structure model. Variable slip model by Sato et al. (2005) is characterized to two asperities and background regions as shown in Fig.1. Table 1 shows analytical condition. The model S51 in Table 1 assumes the point source located within the asperity 1. Since random numbers used in generating time histories are given in advance, synthesized strong ground motions at ASK and ECJ from all four participants coincide with each other. This agreement indicates that the frequency dependent radiation coefficient of the source is properly applied and site response by oblique incidences of both SH and SV is accurately calculated. The model S61 in Table 1 assumes extended source and strong ground motions are synthesized at 4 sites. The response spectra from four participants show good agreement to each other. The response spectra are also compared with those from empirical attenuation model. Although the response spectra shorter than 0.2 sec correspond with each other, the spectra longer than 0.2 sec from stochastic Green's function method show systematically smaller amplitude than that from empirical attenuation model. By comparing the synthesized strong motions from theoretical method such as the wavenumber integration method and thin layer method under the same subsurface structure, the applicability of hybrid approach will be discussed. Please check the following web site for more details.

<http://kouzou.cc.kogakuin.ac.jp/test/home.htm>

### Acknowledgments:

This project is in part supported by a research fund of Ministry of Education, Culture, Sports, Science and Technology of Japan (MIEXT), the Research Subcommittees on the Earthquake Ground Motion of the Architectural Institute of Japan, and the Research Center of Urban Disaster Mitigation (UDM) of Kogakuin University.

### References:

- Kato et al., Benchmark tests for strong ground motion prediction methods: Case for stochastic green's function method (Part 1), AIJ J. Technol. Des. Vol. 17, No.35, 49-54, 2011.
- Kato et al., Benchmark tests for strong ground motion prediction methods: Case for stochastic green's function method (Part 2), AIJ J. Technol. Des. Vol. 18, No.38, 67-72, 2012.
- Sato et al., Earthquake source fault beneath Tokyo, Science, 309, 462-464, 2005.

Keywords: Strong motion prediction methods, Benchmark tests, Stochastic Green's function method, Random numbers, Point source, Fault model

SSS26-03

Room:304

Time:May 20 09:30-09:45

Table 1 Benchmark tests for stochastic green's function method

モデル名	ステップ5 (点震源)		ステップ6 (面震源)	
	S51 (必須)	S52 (必須)	S61 (必須)	S62 (任意)
対象地震	1923年関東地震(Mj7.9)のアスぺリティ		1923年関東地震(Mj7.9)	
震源のモデル化	アスぺリティ内の1要素を点震源として用いる		Sato <i>et al.</i> (2005)のすべり分布の特性化モデル	Sato <i>et al.</i> (2005)のすべり分布を使用した不均質モデル
地盤	関東平野の3次元深部地盤モデル(長周期地震動予測モデル、2009試作版)を用い、観測点直下の平行成層地盤を使用			
減衰	あり			
乱数位相	指定	各自の乱数位相3パターン		
有効振動数	0~20Hz			
出力点	4地点(岩盤サイト:浅川、堆積層サイト:清瀬、越中島、本郷)			

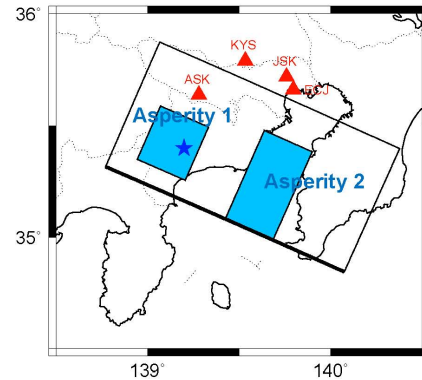


Fig. 1 Characterized fault model and stations for calculation

## Correction for slip function and its implications

MASUDA, Tetsu<sup>1\*</sup>

<sup>1</sup>ERI

Green's function method is useful for simulating strong ground motion. It is necessary to correct for the amplitude and dominant period difference between the bigger target earthquake and the small earthquake as the Green's function. Correction is based on the scaling relations that the slip rise time, as well as slip amount, is scaled by the source dimension. Correction functions of particular type have been proposed. Boxcar type function (Irikura, 1983), exponential time function (Onishi and Horike 2004) for slip velocity time function, or two-order rational function for radiated wave spectrum (Dan and Sato, 1998) is assumed to derive correction function, while Irikura (1986), Irikura et al.(1997), and Nozu (2002) directly specified the correction functions. The correction function spectrum takes a constant value  $N$ , which is the ratio of source dimension, in lower frequencies than a corner frequency  $f_t$  relating to the target rise time  $T$ , and it is unity in higher frequencies than another corner frequency  $f_g$  relating to the small earthquake rise time, and it falls off with increasing frequency between the two corners.

Seismic wave is evaluated by integrating slip velocity over the fault surface. Assuming the slip velocity is uniform over the rectangular fault and rupture propagates constantly, surface integral of slip velocity over a finite fault results in a product of two Sinc functions, one with argument of  $2\pi f T_x$ , and another with argument of  $2\pi f T_y$ , where  $T_x = (X/c - 1/V_x) \cdot L/2$ ,  $T_y = (Y/c - 1/V_y) \cdot W/2$ ,  $f$  is frequency,  $L$  and  $W$  the source dimension,  $X$  and  $Y$  the direction cosine,  $R$  the distance,  $c$  the phase velocity,  $V_x$  and  $V_y$  the rupture velocity. The spectrum is flat in lower frequencies than  $f_c$ , relating to square root of  $T_x \cdot T_y$ , and it falls off from the corner proportionally to the squared frequency.

In Green's function method, instead of integrating slip velocity, waves of small earthquakes located at discrete points are summed up. The spectrum of summation is also flat in lower frequencies than the corner  $f_c$ , and falls off similarly from  $f_c$ , however in this case, it increases from a frequency  $f_e = f_c/N$  and keeps a constant level in higher frequencies.

The corner frequency  $f_c$  is due to fault finiteness, and the spectrum decays from  $f_c$ . If the corner  $f_t$  is close to  $f_c$ , the spectrum of synthesized wave by means of Green's function method falls off between these two corners steeper than the omega-squared model because both of the correction function and summation over the fault. The rise time is in many cases set to  $W/2V_r$  referring to numerical simulations by Day (1982). In this case, the corner frequency  $f_t$  is close to  $f_c$ , and consequently underestimation of spectrum contents is resulted between these two corners. Kataoka et al.(2003) pointed out that the shorter rise time is consistent with the observations.

The rise time  $W/2V_r$  is an approximation of total duration of slip near the center of fault. The slip velocity steeply increases after rupture arrives and decrease in a short time after it reaches the peak, and the peak decreases to zero at fault edge. Many studies of source process indicate that the rise time is as short as one tenth of total duration of rupture  $L/V_r$ .

Uniform slip velocity over an asperity area is usually assumed in a characteristic source model. The rise time  $W/2V_r$  is too long if applied all over asperity area, and shorter rise time is appropriate for the proposed correction functions. The correction function by Onishi and Horike or Nozu is consistent with the impulsive feature of slip velocity. A large value of exponent coefficient is preferable since it approximates the numerical results. In order to properly estimate seismic wave spectrum independent of the size of the Green's function, it is necessary to set a shorter rise time or to take a large value of exponent coefficient.

Keywords: Green' function method, slip time function, correction function, rise time



## Quick estimation of moment magnitude based on real-time displacement waveform

HIRAI, Takashi<sup>1\*</sup>, FUKUWA, Nobuo<sup>1</sup>

<sup>1</sup>Environmental Studies, Nagoya University

### 1. Introduction

The 2011 off the Pacific coast of Tohoku Earthquake was the greatest earthquake in Japan as the magnitude of 9.0. But the first report of JMA (Japan Meteorological Agency) magnitude estimated at 3 minutes after initiation was 7.9. Furthermore, the moment magnitude which should be calculated at 15 minutes after initiation was not calculated due to the saturation of broad-band seismometers. As a result, the tsunami height was underestimated causing loss of many lives unfortunately. Now southwestern Japan faces a great earthquake of Nankai trough, so it is extremely important to construct the quick estimation system of unsaturated magnitude. Previously we developed a method to estimate the permanent displacement accurately based on an acceleration record<sup>1)</sup>. Applying the method, we propose a scheme to estimate moment magnitude quickly using the relation between the displacement and hypocenter distance.

### 2. Method

Relation between the permanent displacement  $u$  due to the earthquake and the hypocenter distance  $r$  is expressed as

$$u = M_0 A / Gr^2, \dots (1)$$

where  $M_0$  is the seismic moment,  $A$  is a coefficient to consider the direction effect,  $G$  is the rigidity. Taking the logarithm of eq. (1), we obtain

$$\log u = -2 \log r + \log (M_0 A / G) \dots (2)$$

Namely, plotting displacements versus hypocenter distances in double logarithmic chart, the seismic moment  $M_0$  can be calculated from the intercept of line of slope -2.

In this study, based on the acceleration waveform recorded by the strong ground motion observation network KiK-net, we obtained the displacement waveform and permanent displacement according to Hirai and Fukuwa (2012)<sup>1)</sup>. Applying this procedure to many observation point, the seismic moment and moment magnitude were calculated.

### 3. Result and discussion

The result for the 2011 off the Pacific coast of Tohoku Earthquake is shown in the Figure. Figure (a) shows the permanent displacement distribution, (b)-(g) show estimated values of the magnitude at each time, respectively. According to the Figure, it is found that the estimated value of the magnitude grows increasingly and that the earthquake can be obtained as  $M_w \sim 9$  class great at 4 minutes after the initiation. This value is consistent with that from the inversion of co-seismic crustal deformation observed by GPS network<sup>2)</sup>. Therefore, the availability of this method was suggested.

### References

- 1) T. Hirai and N. Fukuwa, Estimation of crustal deformation distribution due to the 2011 off the Pacific coast of Tohoku Earthquake based on strong motion records, *J. Struct. Constr. Eng., AIJ*, **77**, 341-350 (2012).
- 2) T. Ito, K. Ozawa, T. Watanabe, T. Sagiya, Slip distribution of the 2011 off the Pacific coast of Tohoku Earthquake inferred from geodetic data, *Earth Planets Space*, **63**, 627-630 (2011).

### Acknowledgment

We used the KiK-net seismograms by National Research Institute for Earth Science and Disaster Prevention.

Keywords: moment magnitude, quick estimation, permanent displacement, strong motion record

SSS26-05

Room:304

Time:May 20 10:00-10:15

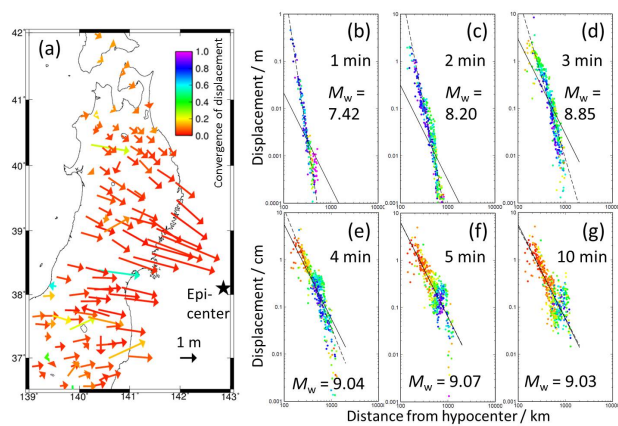


Fig. (a) Permanent displacement distribution. (b)-(g) Real-time magnitude estimation.



## Scaling relations of source parameters for great earthquakes on long active fault systems and plate boundaries

TAJIMA, Reiko<sup>1\*</sup>, Yasuhiro Matsumoto<sup>1</sup>, SI, Hongjun<sup>1</sup>

<sup>1</sup>Kozo Keikaku Engineering Inc.

We investigated seismic scaling relations of rupture area (S), average slip (D), combined area of asperities (Sa) and short-period source spectra (A) versus seismic moment (Mo) for 6 crustal earthquakes with Mw >= 7.5 on long active fault systems and 6 plate-boundary earthquakes with Mw >= 8.4, to examine the validity of the scaling relations derived by past-study, and to understand the difference between source parameters derived from long-period source models with heterogeneous slip and short-period characterized source models. This study is a part of results of the contract study "Comparative study of scaling relations of source parameters for great earthquakes on long active fault systems and plate boundaries" from the Nuclear Safety Commission of Japan.

For the crustal earthquakes we found that the Mo-S relation fits in the line derived by Murotani et al. [2010] which is assuming a proportion to Mo<sup>1</sup> (Figure. 1a). The relationship corresponds to the third stage in 3 stage scaling model [Irikura et al., 2004] which is caused by the saturation of maximum displacement (Dmax) at approximately 10 m. This is also confirmed in our result of the Mo-Dmax relation. The Mo-Sa relation derived from long-period and short-period models are similar to each other. The S-Sa relation seems to fit in the scaling relation suggested by Somerville et al. [1999]. The Mo-A relation is within a scattering of relationship by Dan et al. [2001].

For the plate-boundary earthquakes we found that the Mo-S relation is clearly smaller than that by Murotani et al. (2008) for the M9 events. We also found that the fault widths seem to saturate at approximately 200 km from our results. Then we derived the following new scaling relation S and Mo for great plate-boundary earthquakes with Mw >= 8.4 (Mo >= 4.4 x 10<sup>22</sup> Nm) assuming a proportion to Mo<sup>1/2</sup>:

$$S \text{ (km}^2\text{)} = 5.88 \times 10^{-7} \times Mo^{1/2} \text{ (Nm)} \dots\dots\dots (1).$$

This corresponds to the second stage in the 3 stage scaling model that is caused by the saturation of fault width due to the restriction of the seismogenic layer in the subduction-zone. We also confirmed that D and Dmax are not saturated, i.e. the relation does not arrive at the third stage in the 3 stage scaling model yet. The Mo-Sa and S-Sa relations derived from long-period models fit in the scaling relations suggested by Murotani et al. [2008]. However the Mo-Sa relation derived from short-period models is 2.5 times as small as that of long-period models, and matches the scaling relation by Sato [2010] using the plate-boundary earthquakes. The Mo-A relation is higher than that by Dan et al. [2001] using the crustal earthquakes, but fits in the relation by Sato [2010] using the plate-boundary earthquakes. We think that it is important to accumulate more source models with the different period range because we could discuss about only the 2011 Tohoku earthquake for the plate-boundary earthquake in this study.

Keywords: great earthquake, source parameter, source model, scaling, asperity, rupture area

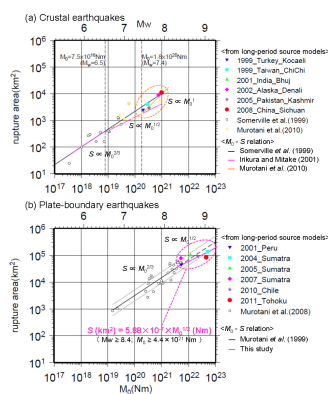


Figure 1. Relation between rupture area (S) and seismic moment (Mo).

## Simulation of strong ground motions from the 2011 Tohoku earthquake and a recipe of predicting strong ground motions for

IRIKURA, Kojiro<sup>1\*</sup>, KURAHASHI, Susumu<sup>1</sup>

<sup>1</sup>Aichi Institute of Technology

### 1. Introduction

Source models of the 11 March 2011 mega-thrust earthquake with Mw 9.0 off the Pacific coast of Tohoku have been investigated by many authors using variety of data-sets from very long-period data such as GPS and Tsunami to short-period data such as teleseismic short period P waves and strong ground motion data. The main slip distributions from very long-period data were located east of the hypocenter toward the Japan Trench zone (Ozawa, et al., 2011 and Fujii and Satake, 2011). A unified source model was constructed through joint inversion of teleseismic, strong motion, and geodetic datasets by Koketsu et al. (2011) and Yokota et al. (2011). They showed that the main rupture propagated not only in the strike direction but also in the dip direction and included both the deep area called the Miyagi-oki region and the compact shallow area near the Japan Trench. On the other hand, we made a source model for generating short-period ground motions comparing observed strong motions with simulated ones using the empirical Green's function method. Our results showed that strong motion generation areas located along the down-dip edge of the source fault. Koper et al. (2011) found the frequency-dependent rupture process of the 2011 Mw 9.0 Tohoku Earthquake comparing source models using backprojection (BP) imaging with teleseismic short-period (<1 s) P waves, and finite faulting models (FFMs) of the seismic moment and slip distributions inverted from broadband (>3 s) teleseismic P waves, Rayleigh waves and regional continuous GPS ground motions. Their results showed indicate that the down-dip environment radiates higher relative levels of short-period radiation than the up-dip regime for this earthquake.

That is, the source models summarized above have common features of the source models that the main slip distributions from the long-period data were located east of the hypocenter toward the Japan Trench zone, while short-period generation areas located west of the hypocenter. These results are not consistent with the basic idea of the recipe of predicting strong ground motions developed based on slip distributions from the waveform inversions for inland crustal earthquake with M 7 class. The recipe was so far constructed based on an idea that large slip areas coincide with strong motion generation area.

In this study, we first summarized source models for generating strong ground motions and then propose an improved idea for recipe of predicting strong ground motions for mega-thrust earthquakes.

### 2. Source models of strong ground motions

We estimate a source model for generating strong ground motions from this earthquake using the characterized source model. Five wave-packets in the observed seismograms were identified, which originated from five strong motion generation areas (SMGAs) on the source fault. The locations of the SMGAs are constrained using the back-propagation method of Kurahashi and Irikura (2010).

Then we obtain the final solutions for the area and initiation point by comparing the observed seismograms of each wave-packet and the synthetic ones at many stations using a trial and error approach. Locations of those five SMGAs seem to correspond to source segments divided for past seismic activity in the region off the Pacific coast of Tohoku by the Headquarters for Earthquake Research Promotion of Japan (HERP). SMGA 1 is located in the source region of Southern Sanriku-oki west of the hypocenter and SMGA 2 in that of the Middle Sanriku-oki north of the hypocenter. SMGA3 is located in the source region of the Miyagi-oki, SMGA 4 is located in that of Fukushima-oki and SMGA 5 is located in that of Ibaraki-oki.

These results suggest a way how to locate such strong motion generation areas for predicting strong ground motions from the mega-thrust earthquake.

### 3. Methodology of predicting strong ground motions for mega-thrust earthquake.

Detailed methodology of predicting strong ground motions is introduced in the session.

Keywords: great earthquake, source parameter, source model, scaling, asperity, rupture area

## Strong motions from the 2007 Niigata-ken Chuetsu-oki earthquake based on characterized source model with super-asperity

SHIBA, Yoshiaki<sup>1\*</sup>, HIKIMA, Kazuhito<sup>2</sup>, UETAKE, Tomiichi<sup>2</sup>, TSUDA, Kenichi<sup>3</sup>, HAYAKAWA, Takashi<sup>3</sup>, Shinya Tanaka<sup>4</sup>

<sup>1</sup>CRIEPI, <sup>2</sup>TEPCO, <sup>3</sup>ORI, <sup>4</sup>TEPCO

Strong motion records of the 2007 Niigata-ken Chuetsu-oki earthquake were obtained at several observation stations in the Kashiwazaki-Kariwa (KK) NPP site. Three distinctive pulse waves are observed in common among these main-shock records, thus they were considered to be radiated from three asperities on the fault plane. On the other hand the observed velocity amplitude of third pulse shows large variation among stations distributing within several hundred meters. Since the base mat of the reactor building where the seismometer is installed is located on bedrock, such variation of observed ground motions cannot be attributed to local site response estimated from shallow subsurface structure. Shiba et al. (2011) calculated the third pulse by using the finite difference method with 3-D deep subsurface velocity model; however the difference of pulse amplitude could not be sufficiently derived by assuming characterized source model. In this study we examine the detailed wave propagation from the asperity generating third pulse (i.e. third asperity) to KK-NPP site by dividing the asperity area into small sub-areas, and find that the variation of third pulse's amplitude becomes apparent when the seismic waves are radiated from only the southwestern part of the asperity. Source inversion analysis simultaneously searching the slip and the peak slip rate also shows locally high slip rate at the southwestern corner of the third asperity. Thus we assume the characterized source model having the super-asperity with relatively high stress drop on the southwestern corner of the third asperity, and carry out the broadband strong-motion simulation at the KK-NPP site. As a result the observed third pulse waveforms for the EW component are successfully reproduced including the quantitative variation. However for the NS component the fit between the observed and the synthetic pulses are insufficient. In the characterized source model the spatial variation of the rake angle on the fault plane is not taken into consideration, and it might cause the different goodness of fit between two horizontal components.

Keywords: the 2007 Niigata-ken Chuetsu-oki earthquake, characterized source model, strong-motion simulation, super-asperity, source inversion

## Revision of seismic hazard assessment after the 2011 Tohoku earthquake

FUJIWARA, Hiroyuki<sup>1\*</sup>, MORIKAWA, Nobuyuki<sup>1</sup>, OKUMURA, Toshihiko<sup>2</sup>

<sup>1</sup>NIED, <sup>2</sup>Shimizu corp.

The Tohoku-oki earthquake (Mw 9.0) of March 11, 2011, was the largest event in the history of Japan. This magnitude 9.0 mega-thrust earthquake initiated approximately 100 km off-shore of Miyagi prefecture and the rupture extended 400 - 500 km along the Pacific plate. Due to the strong ground motions and tsunami associated by this event, approximately twenty thousand people were killed or missing and more than 220 thousands houses and buildings were totally or partially destroyed. This mega-thrust earthquake was not considered in the national seismic hazard maps for Japan that was published by the headquarters for earthquake research promotion of Japan (HERP). By comparing the results of the seismic hazard assessment and observed strong ground motions, we understand that the results of assessment were underestimated in Fukushima prefecture and northern part of Ibaraki prefecture. Its cause primarily lies in that it failed to evaluate the M9.0 mega-thrust earthquake in the long-term evaluation for seismic activities. On the other hand, another cause is that we could not make the functional framework which is prepared for treatment of uncertainty for probabilistic seismic hazard assessment work fully. Based on the lessons learned from this earthquake disaster and the experience that we have engaged in the seismic hazard mapping project of Japan, we consider problems and issues to be resolved for probabilistic seismic hazard assessment and make new proposals to improve probabilistic seismic hazard assessment for Japan.

After the Tohoku-oki earthquake, HERP had been reviewing the long-term evaluation for the area in which the Tohoku-oki earthquake occurred and released the revised version of the "Long-term evaluation of seismic activity for the region from the off Sanriku to the off Boso" in November 2011. In this revision, although the revision of the methodology of the long-term evaluation itself has not yet been made and the most part has remained a traditional evaluation, a new assessment has been made of the Tohoku-oki type earthquake. Based on this evaluation, we have been making a revision of the seismic hazard assessment. In this revision, not only results of the long-term evaluation have been revised, but also the upper limits of background earthquakes have been revised. In addition, here we propose three models in order to consider uncertainty of seismic activity.

We also have prepared the maps that show the strong-motion level for earthquake preparedness. For example, based on the averaged long-term seismic hazard assessment, evaluating strong-motion level for 5,000, 10,000, 50,000, 100,000 years return period, we have made the maps that show the distribution of strong-motion level, which represent effect of major earthquakes on active faults and subduction zone earthquakes with low-probability.

Keywords: National Seismic Hazard Maps, strong-motion, seismic hazard, probability

## Change in site amplification factors before and after the 2011 Off Tohoku earthquake

TAKEMOTO, Teito<sup>1\*</sup>, FURUMURA, Takashi<sup>2</sup>, MAEDA, Takuto<sup>2</sup>

<sup>1</sup>Earthquake Research Institute, the University of Tokyo, <sup>2</sup>Center for Integrated Disaster Information Research, Interfaculty Initiative in Information Studies

### **Introduction**

We have compared between estimated broad band site amplification factor before and after the 2011 Off Tohoku earthquake at each site of the K-NET, KiK-net and F-net strong motion network in Japan. The amplification factors are estimated by coda normalization method (e.g. Phillips and Aki, 1986).

Estimated amplifications are applied for shaking intensity to show the validity of our estimates on the site amplification factors at each site and in frequencies (Takemoto et al., 2012 in press). In this paper, we also found even KiK-net borehole stations have strong site effect.

In this study, we confirmed that site amplification over 4 Hz significantly drops after 2011 Off Tohoku earthquake.

### **Data and Method**

We used KiK-net surface and borehole stations and F-net nation-wide strong motion network developed across Japanese Islands. Using waveform data of acceleration record from 48 moderate earthquakes, we estimated the site amplification characteristic at each station in four frequency bands ( $f = 0.5-1$  Hz,  $1-2$  Hz,  $2-4$  Hz, and  $4-8$  Hz).

The distribution of the site amplification characteristic in each frequency bands has been estimated by inversion. We assumed an F-net broadband seismic observation station installed in the basement rock site as unity (0 dB) site amplification. We also estimate site amplification after 2011 Off Tohoku earthquake using 4 events in northeastern Japan.

### **Results**

In the high-frequency band ( $f = 0.5-1$  Hz), we cannot confirm change of site amplification after the Tohoku earthquake. In the high frequency band ( $4-8$  Hz), site amplification factors in most stations drop around half value.

Site amplification from coda normalization method is value relative to one F-net station. If absolute site amplification in F-net increase, site amplification factor of all stations will drop. For check the change of site amplification without certain reference, we compared two acceleration waveform at FKS006, where site amplification largely drop after Tohoku quake, and FKSH09, where site amplification drop small, in two quakes that location and mechanism are similar each other. Hypocentral distance from two events to stations are almost same. In 2010 event, amplitude at FKS006 is larger than FKSH09 by over seventh. This indicate site amplification in FKS006 is much larger than FKSH09. On the other hand, in 2011 event, amplitude at FKS006 is about twice to FKSH09. Therefore, we can confirm change of the site amplification from waveform. We will estimate the change of site amplification more quantitative in future study.

### **Acknowledgement**

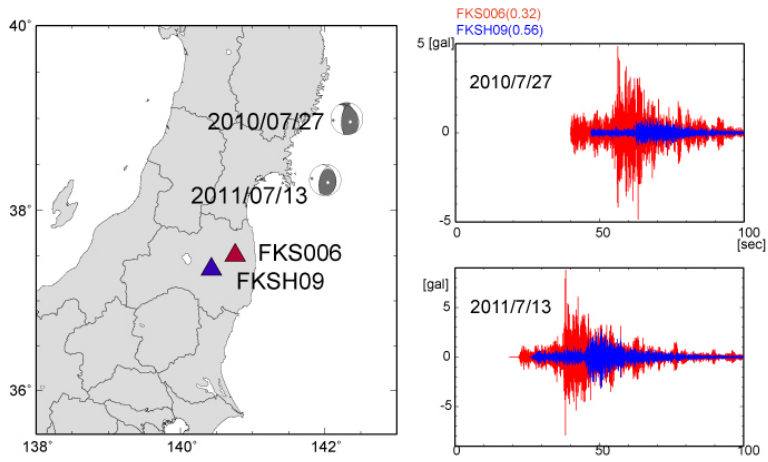
We acknowledge the National Research Institute for Earth Science and Disaster Prevention, Japan (NIED) for providing the K-NET, KiK-net and F-net waveform.

Keywords: 2011 Off Tohoku earthquake, site amplification

SSS26-10

Room:304

Time:May 20 11:45-12:00





## Development of a new ground motion prediction equation applicable up to Mw9 -evaluation of additional correction terms-

MORIKAWA, Nobuyuki<sup>1\*</sup>, FUJIWARA, Hiroyuki<sup>1</sup>

<sup>1</sup>NIED

We have proposed a new ground motion equation in Japan directly applicable up to Mw=9 by using strong motion data of the 2011 Tohoku-oki earthquake. The equation is a simple base model using only two parameters, Mw and closest distance to the source fault. In this study, we obtain following three additional correction terms applied to the above basic equation. The first is the term for amplification due to deep sedimentary layers. We investigate the relation between the amplification and top depth of each layer using the deep subsurface structure model by Fujiwara et al. (2009). The second is the term for amplification due to shallow soil structures using the average S-wave velocity up to 30m depth as a parameter. The third is the term for anomalous seismic intensity distribution using the closest distance from the volcanic front to target site as a parameter.

Keywords: ground motion equation, strong motion, site amplification, anomalous seismic intensity distribution

## Building Damage Ratios and Ground Motion Characteristics during the 2011 off the Pacific coast of Tohoku Earthquake

WU, Hao<sup>1\*</sup>, MASAKI, Kazuaki<sup>2</sup>, IRIKURA, Kojiro<sup>3</sup>, WANG, Xin<sup>3</sup>, KURAHASHI, Susumu<sup>3</sup>

<sup>1</sup>Graduate School of Engineering, Aichi Institute of Technology, <sup>2</sup>Department of Urban Environment, Aichi Institute of Technology, <sup>3</sup>Disaster Prevention Research Center, Aichi Institute of Technology

The relationship between building damage ratios and ground motion characteristics, such as peak ground accelerations (PGAs), peak ground velocities (PGVs), JMA seismic intensities (LJMAS), spectral intensities (SIs), acceleration response spectra (Sa) and pseudo velocity response spectra (pSv) was discussed for the 2011 off the Pacific coast of Tohoku Earthquake. In this study, damage ratio is defined as the ratio of the number of damaged buildings including collapsed, half-collapsed and partially damaged ones, to the total number of buildings in each district (an administrative unit, such as a city, or town). The damage statistics were obtained from the Fire and Disaster Management Agency published on January 13, 2012. The districts mainly damaged by tsunami were excluded. It was found that DRs correlated better with velocity indices such as PGVs, pSv and SIs than acceleration ones such as PGAs, Sa and LJMAS, and DRs correlated better with pSv at 0.5 s than those at 1.0 s and 1.5 s from the view of coherence coefficients. In general, DRs tended to increase with the level of ground motion characteristics, but the damage ratios in some districts did not correspond to suitable level of ground motion characteristics. It was suggested that the ground motion characteristics at the K-NET and KiK-net stations might not represent those in the damaged districts because the stations are far away from the damaged areas.

In order to establish the relationship between building damage ratios and ground motion characteristics in the damaged areas, the estimations of ground motion at the damaged sites were performed based on microtremor measurements. They were accomplished by the product of bedrock motions and site amplification factors at the damaged sites. The ground motions on bedrock under damaged sites and observation stations were assumed to be the same. The bedrock motions under the damaged sites were estimated from observation spectra on surface divided by site amplification factors at the observation station. Then the ground motions were estimated from the product of the bedrock motions and site amplification factors at the damaged sites. Therefore, it was necessary to find the subsurface S-wave velocity structures both at the observation station and damaged site to estimate site amplification factors. Based on one dimensional Haskell multiple reflection theory, the S-wave velocity structures were obtained by inversion of the microtremor H/V spectral ratios. We conducted microtremor measurements and building damage survey at the observation station and the damaged sites. The H/V spectral ratios of microtremor at the observation station showed good consistency with those of ground motions from small earthquakes, which indicated that the inversion of microtremor H/V spectral ratios was feasible, just as the seismic motion ones. The ground motion characteristics at the damaged sites estimated by the above procedure were related with the damage ratios.

Keywords: ground motion characteristics, building damage ratio, S-wave velocity structure, H/V spectral ratio

## Shear-Wave Velocity Evaluation from Microtremor Records Measured in a Damaged Nine-Story SRC Building

WANG, Xin<sup>1\*</sup>, MASAKI, Kazuaki<sup>2</sup>, IRIKURA, Kojiro<sup>1</sup>

<sup>1</sup>Disaster Prevention Research Center, Aichi Institute of Technology, <sup>2</sup>Department of Urban Environment, Aichi Institute of Technology

The building analyzed in this paper is a severely damaged nine-story steel reinforced concrete (SRC) building during the 2011 off the Pacific coast of Tohoku Earthquake, which was designed and constructed in 1990 according to the new anti-seismic design code of Japan. Hereafter it is called K9SRC for short. Obvious shear cracks happened in the external concrete walls in the longitudinal direction (EW), which can be defined as non-structural damage. However, the shear deformation of walls brought about distortion of entrance doors, which hindered escape during the earthquake. The building K9SRC suffered structural damage in the northwest corner column of the first story and multistory shear walls of lower stories, whose steel bars have yielded and been exposed to air. After the earthquake, the building K9SRC was classified to be dangerous. Residents have to move out until it is repaired.

According to the preliminary reconnaissance report of the 2011 Tohoku-Chiho Taiheiyo-Oki Earthquake published by the Architectural Institute of Japan, buildings constructed after 1981 generally showed a good performance during this earthquake, and few of them suffered severe damage. Furthermore, based on the on-site investigation performed by our study group, there are no buildings damaged as severely as the building K9SRC within 1000 km of it. Therefore, the building K9SRC should be paid more attention to scrutinize the damage of it.

In this paper, we made comparative observations of microtremors on each floor and the top of the building K9SRC to extract the shear-wave velocity ( $V_s$ ) traveling within each story using the deconvolution method. Because the shear wave velocity relates only with the seismic property of the structure, it is a reliable way to evaluate the inter-story shear stiffness degradation.

Based on the analyses,  $V_s$  decreases more greatly in the longitudinal direction than in the transverse direction. The interfloor  $V_s$  in the longitudinal direction has decreased to less than 300 m/sec. In the transverse direction, the  $V_s$  decrease along the height of the building, and  $V_s$  traveling in the lower four stories are higher than 300 m/sec.  $V_s$  traveling within the first story decreased obviously because of the damage of the corner column. The  $V_s$  traveling within the 5th and 6th story decreased to less than 300 m/sec in both of the longitudinal and transverse direction.

Keywords: shear-wave velocity of buildings, deconvolution method, microtremor measurement, damaged building

## Continued effort for the Development of the i-Jishin cloud system

AZUMA, Hiroki<sup>1</sup>, NAITO, Shohei<sup>1\*</sup>, FUKUMOTO, Rui<sup>3</sup>, NAKAMURA, Hiromitsu<sup>1</sup>, SENNA, Shigeki<sup>1</sup>, FUJIWARA, Hiroyuki<sup>1</sup>, YOSHIDA, Minoru<sup>2</sup>

<sup>1</sup>National Research Institute for Earth Science and Disaster Prevention, <sup>2</sup>Hakusan Corporation, <sup>3</sup>Wingbase Inc.

Yoshida et al. (2011) developed an experimental sensor network of earthquake observation using iPhone/iPad/iPod-touch named i-Jishin, and released at App Store in August, 2010.

We introduce after works on this session.

Keywords: i-Jishin, Application, ground motion measurement, cloud, sensor, disaster prevention

